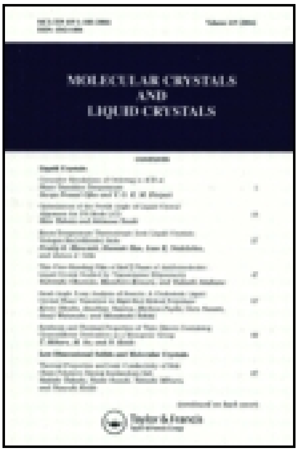

Molecular Crystals and Liquid Crystals
Publication details, including instructions for authors and subscription information:
http://www.tandfonline.com/loi/gmcl20

Tunable Non-locality of Thermal Non-linearity in Dye Doped Nematic Liquid Crystal

J. F. Henninot [a], M. Debailleul [b] & M. Warenghem [b]
[a] LPCIA Faculté J. Perrin, Université d'Artois, rue J. Souvraz SP18, LENS Cedex, 62307 E-mail:
[b] LPCIA Faculté J. Perrin, Université d'Artois, rue J. Souvraz SP18, LENS Cedex, 62307

Version of record first published: 18 Oct 2010

To cite this article: J. F. Henninot, M. Debailleul & M. Warenghem (2002): Tunable Non-locality of Thermal Non-linearity in Dye Doped Nematic Liquid Crystal, Molecular Crystals and Liquid Crystals, 375:1, 631-640

To link to this article: http://dx.doi.org/10.1080/10587250210613

Mol. Cryst. Liq. Cryst., Vol. 375, pp. 631-640

1058-725X/02 $12.00 + .00

Tunable Non-locality of Thermal Non-linearity in Dye Doped Nematic Liquid Crystal

J. F. HENNINOT, M. DEBAILLEUL and M. WARENGHEM

LPCIA Faculté J. Perrin, Université d'Artois, rue J. Souvraz SP18 62307 LENS Cedex, E-mail: henninot@univ-artois.fr

In this paper we report on experiments performed to estimate the non-locality of the photothermal non-linearity in thick dye-doped nematic liquid crystal (DDNLC). We have studied the interaction of two counter-propagating self-focused laser beams parallel to each other. From this experiment, a rough estimation of the width of the induced index profile with respect to the beam size is derived (non-locality). In a second part, we report a set of results concerning the tuning of this non-locality. As the laser light is chopped and for power large enough, the beam is self-trapped in a narrow isotropic channel, the length of which depends on the input power. We describe an original experiment of self-guiding of light by the use of such an effect, namely bent isotropic channels.

Keywords thermal lensing, self-waveguiding, optical soliton, non-locality

INTRODUCTION

A number of non-linear optical phenomena can be induced by laser-heating effects as the thermal lens effect [1] and the formation of isotropic holes in nematic [2]. In the case of laser-heating induced refractive index change, the process may not be exactly described by a Kerr-like law. The thermal non-linearity is non-local as connected to a diffusion process, which takes place predominantly along the radial

coordinates of the beam. Thermal effects induced by light in Liquid Crystals (LC) materials have been studied, especially for optical limiting purposes [3]. Nevertheless, in most of the experiments, the length of interaction between the beam and the LC is rather small, of the order of the size of the laser beam. A few years ago, we have described an experiment of laser beam self-trapping in dye doped nematic liquid crystal. We have shown that it was possible to obtain a soliton-like propagation over 9 or 10 diffraction lengths, explaining this effect by involving the strong thermal non-linearity exhibited by the LC when a small part of the laser beam was converted to heat by absorption by the dye (0.1% in weight in the LC)[4]. Two different propagation regimes have been reported and are reminded respectively in the first and second parts, they both are due to thermal non-linearity [5].
In this paper, we mainly address the concept of non-locality in the observed thermal self-focusing effects from an experimental point of view: the thick DDNLC samples are a good tool to undertake such an analysis and comparison with more theoretical approaches [6]. In the first part of this paper, we report on a rough experimental estimation of the index profile width (non-locality) obtained in the first soliton-like regime. In the second part, we report on a way to control the non-locality in the second soliton like regime (isotropic tube) and a using of it in steering light.

1. Non-locality probed using quasi-soliton deflection

As two bright solitons are mutually coherent, the interaction force between them can be attractive or repulsive, depending on their relative phase [7]. In the case of thermal non-linearity [8], they are unaltered on collision and they never repulse one from each other.
As already mentioned by Mitchell [7], the interaction of spatial solitons can be described by using a topological analogy. In this frame, the beams can be compared as particles that are influenced by the potential curve (in fact, the index profile) generated by the other beam. In other words, a beam can be deflected as it enters an index gradient generated by another beam. Obviously, the deflection is correlated to the index gradient and a measurement of this deflection reveals the index profile. In the case of an absorbing media, the intensity of a beam decreases along the propagation direction, the induced index profile changes as well. We have taken advantage of this feature to generate an asymmetric profile along the z-axis, using two counter-propagating

beams, collimated in its first soliton-like regime (Figure 1). In this geometry, the less intense part of one beam is deflected by the intense part of the other one, increasing the sensitivity of the measurement. The experimental trajectories of beams (as sketched on the figure 2) are thus analysed and used to model the index profile.

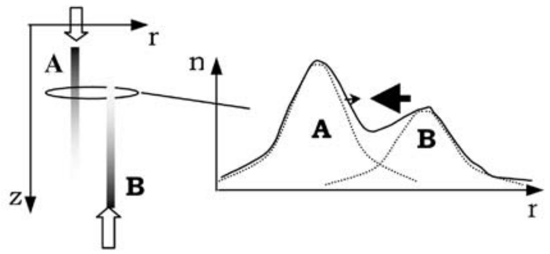

FIGURE 1. Particles-like interaction of collimated beams and index profiles.
Contribution of each beam: dashed lines
Overall index profile : bold line
The white arrows represent the direction of propagation of the light

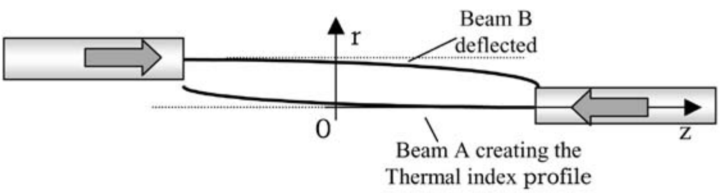

FIGURE 2. Mutual deflections of the beams A and B. (the arrows indicate the direction of propagation for the light).

Let us now consider the Eikonal equation (1) which describes the path of a light ray in an inhomogeneous medium characterised by an index n(r).

$$\frac{d}{ds}\left[n\frac{dr}{ds}\right]=\mathrm{grad}(n) \qquad (1)$$

From experimental observations, the paraxial approximation applies, thus d/ds ≈ d/dz. The absorption being low, it is possible to neglect the second derivative d^2r/dz^2 . The expression (1) reduces to :

$$\frac{dn}{dz}.\frac{dr}{dz}=\frac{dn}{dr} \qquad (2)$$

From the knowledge of the temperature dependence of the ordinary index and a rough estimation of the temperature decrease along with the propagation direction, dn/dz can be estimated over the total length of propagation. The experimental estimation of dr/dz is derived from the measurement of δ for different distances d between the beams (Figure 3) and leads to the determination of the radial index variation dn/dr using (2).

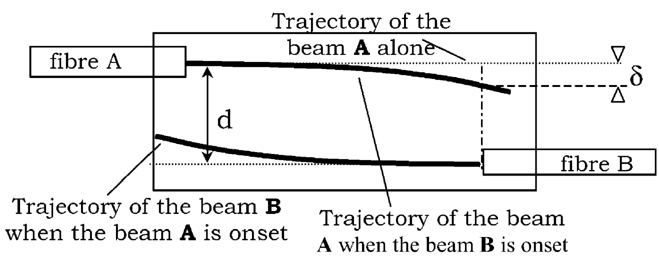

FIGURE 3. Schematic view of the interaction between the two collimated beams. δ is the typical transversal shift of a beam.

<u>Experiments</u>

First, we briefly remind the geometry of the experiment for a single beam we have used to observe the two soliton-like propagation regimes, since we use a similar set up to perform the mutual deflection experiments. The set up is depicted on the figure 4. A 160 μm thick cell is filled with a mixture of the nematic liquid crystal (NLC) 5CB and quinizarine dye in 0.2% concentration by weight. The NLC optical axis is aligned perpendicular to the beam polarisation axis by an electric field. In this case, the ordinary index is involved and due to its positive variation with the temperature, it induces the focusing of the beam. The 532 nm line of an $NdVO_4$ laser emerging out of a single mode fibre

($Ø_{core}$= 3.1 μm, cut-off = 380nm) is used as the light source. The fibre delivers a nearly gaussian beam with a linear polarisation parallel to the x-axis. The radius of the beam is about 1.5 μm. The light enters the cell parallel to the z-axis. All the experiments were performed at room temperature of about 22°C. The dependence of the ordinary index with the temperature ranges from 10^{-3}/°C at room temperature to 10^{-2}/°C close to the nematic to isotropic transition; T_{NI} = 35.5°C).

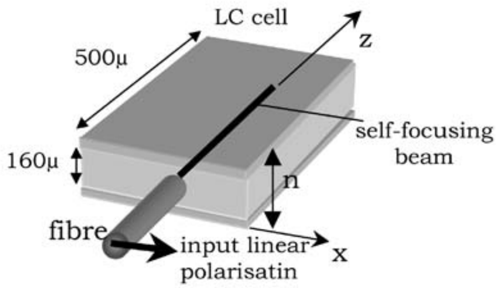

FIGURE 4. Experimental set-up to observe the self-focusing effect

As the source power at the end of the fibre is increased, two major events occur at two different ranges of input power [5]. In this part, we focus on the low power event: the second one will be described in the next part dealing with isotropic tubes.
For an input power around 2mW, it is possible to observe the collimation of the beam over a length of propagation which exceeds 500 μm. The collimation effect, which recalls the phenomenon of spatial soliton observed in photorefractive materials, is observed on 9 to 10 diffraction lengths. Looking carefully the beam at the output of the fibre, we can observe that the collimation starts effectively after a free expansion length of about 50μm (Figure 5).

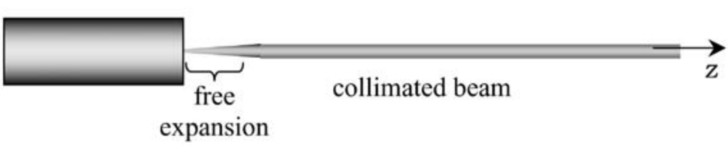

FIGURE 5 Shape of the collimated beam with its free expansion region at the beginning

We have performed some simulations which show that this effect can be explained by the change of thermal conductivity between the DDNLC volume and the glass of the fibre. This difference induces a heat flow from the LC to the fibre and then a slight decreasing of the temperature at the entrance of the sample [9]. The temperature gradient needed to obtain the collimation of the beam is then obtained after the fibre tip. As a consequence, the radius of the collimated beam is slightly larger than the beam guided by the fibre source. We have estimated the value of this radius to be $\omega = 3\mu m$.
The experimental set-up designed to observe the interaction of two collimated beams is similar to that described on the figure 4, apart that now, two fibres are introduced in the cell, face-to-face, as sketched on the figure 3. The fibres position was controlled by 3-stages micropositionners on each side of the cell. The deflection of the beams from their initial direction (without the influence of the neighbour beam) was observed by the means of a microscope associated with a CCD camera. We have measured the mutual deflection of the beams for different transverse distances between the fibres (d, Fig. 3). The temperature on the axis of the beams being close to the NI temperature, the two beams cannot be brought too close from each other, otherwise an overlapping of the two profiles induces a highly unstable thermal equilibrium. For an optimised distance of about 400 μm between the tips of the fibres, we finally found that it was possible to observe steady state deflections for transverse distances d from 10 to 40 μm between the beams. For these transverse distances, only the second half of the beams was significantly deflected. We have measured the overall transverse shift δ of one beam and reported the obtained values in the table 1. The average slope of the deflected beam can then been estimated and introduced as dr/dz in the Eikonal equation (2). The variation of the index with z (dn/dz) can be approximated to a linear decay, taking into account the low absorption coefficient. The maximum temperature at the top of the laser beam intensity profile has been estimated by a finite element modeling. The values of the index variation obtained by this method have been summarised in the figure 6 to shape the index profile experienced by the deflected beam. This profile is not exactly the profile of a beam alone but can be defined as an overall index profile due to the perturbation of the other one. The index profile that would have been generated by a single beam can be deduced from this "perturbed" experimental profile (dashed curve, Figure 6).

$D\ (\mu m)$	$\delta\ (\mu m)$
10	4
15	7
20	2
25	2
30	2

TABLE 1 Transversal shift δ (see Fig. 3) of the beam for different values of d.

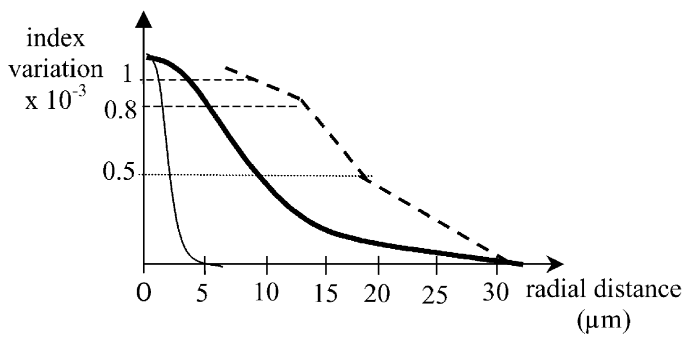

FIGURE 6. Experimental index profile obtained from the Eikonal equation (dashed line: overall index variation profile, bold line: corrected index variation profile, thin line: intensity profile)

To estimate the influence of the overlap in the area around the first beam, we have simulated numerically the interaction between two heat sources. We have chosen a gaussian function for the transverse profile of each source to reproduce as much as possible the laser intensity profile. We have computed the temperature profile and we have compared it to the profile produced by a single beam. By this comparison, it was then possible to generate an error function which reproduces the shift observed between the real and overall index profiles. The corrected index profile appears on the Figure 6 in bold line. For the sake of comparison, we have also reproduced the averaged intensity profile of the collimated beam. The index profile appears to be clearly widerthan the intensity profile. We check here that the thermal effect induced in a thick NLC sample is an highly non-local effect, as it was defined by Krolikowsky and co. [8]. Moreover, we put some figures on this non-locality: the effect is found to be around three times wider than the cause. The transverse diffusion of the heat induces a broadening of the profile, which acts probably as a stabilisation of the self-focusing process.

2. Self trapping of light in a isotropic channel

Coming back to the experiment performed on the set-up described on the figure 4, as already said, we have observed two different events as the input beam power is increased. The second event occurs for a power of the source of around 4 mW. The thermal self-focusing effect overcomes the diffraction and the beams exhibits a focal point. This focal point grows quickly at constant input power to become an elongated isotropic channel in which light is trapped. As the power is slightly increased or decreased, the channel lengthens or shortens reversibly. In order to balance the overall heat transfer of our device (input heat generated by the dye absorption and heat expelled out of the cell), thus to stabilise the temperature field and therefrom the index profile, the input laser light is pulsed. A pretty good balance can be obtained by adjusting the input power, the pulse duration and the repetition rate and it is possible to observe the modes for hours. For the higher input powers (second mode), the isotropic tube is thus well stabilised, with a radius slightly larger than the one of the first mode and which looks like a virtual waveguide. As already said, the length of this channel is correlated to the input power, the radius can be tuned by varying the pulses parameters. With an experimental ratio of 1/10 (on/off time), it is possible to adjust the length of the channel, up to 200μm by increasing of the power.

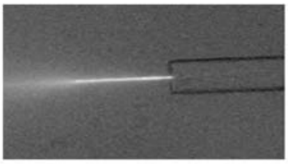

PICTURE 1. Localised NI transition induced by a pulsed laser beam

We have developed an experiment to test the transmission properties of the isotropic channel structure previously described. Using a similar set-up as the one shown on the Figure 4 and with a face to face geometry for the fibres as shown on the Figure 3, we have launched two isotropic channels in opposite directions by injecting a pump laser beam into the two fibres, tilted with respect to each other. As previously said, it is possible to adjust the length of the isotropic channel by varying carefully the input power: this has been done for each source in order to perform a junction between the two channels (Picture 2). A low power He-Ne beam is injected in one of the fibre sources and detected via a lock-in amplifier at the output of the other fibre. We can thus check whether or not the obtained bent structure can guide that light. The distance along z-axis between the fibres was in the order of 400 μm. Using two micropositionners, the angle between the two fibres can be adjusted. By varying this angle, we have checked which maximum bending of the isotropic channel still allows a transmission of the probe beam via the bent wave-guide. As the angle between the two fibres is too large, the probe beam "leaks" out of the first channel and is no longer guided up to the second fibre. The limit is imposed by the index variation induced by the NI transition. We have experimentally found that the probe signal was transmitted through the bent structure and thus it behaves as a wave-guide. The probe signal has been detected at the second fibre output for a maximum angle value of 7 degrees. A rough calculation, based on total internal refraction considerations, shows that this limit angle of 7 degrees yields to an index variation of about 10^{-2}, which is consistent with the known values for the considered material (@ T = 35.3°C and $\lambda = 0.6328\mu m$, $n_o = 1.548$ and $n_{iso} = 1.585$).

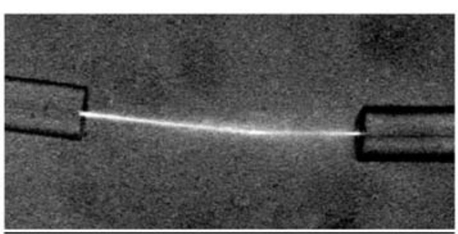

PICTURE 2. Junction established between two counter-propagating isotropic channels. The angle between them is about 7 degrees. Probe light is found to be driven through this bent wave-guide.

Conclusion

In this work, we have developed an experimental method to estimate the width of the thermal indexing in a DDNLC sample excited by a narrow laser beam. This method was based on the deflection of two beams by each other. After a numerical treatment, we have deduced from this experiment the shape of the index profile induced by a beam and we have checked the high non-local behaviour of this non-linear effect. We have then driven this non-locality by controlling the exposure time by the laser light. We have generated a narrow isotropic channel within the NLC medium. We have tested the guiding properties of this channel and we have shown that it can be used in optical connection devices. In a future work, we will study in detail the dynamics of the self-focusing effect to control furthermore its stability.

Acknowledgements

The LPCIA participates to the Centre d'Etudes et de Recherches Lasers et Applications (CERLA) supported by the ministère chargé de la Recherche, the region Nord- Pas de Calais and the Fonds Européen de Développement Economique des Régions.

REFERENCES

1. Th. Graph, E. Wyss, M. Roth, H.P. Weber, Opt. Comm. **190**, pp 327-331 (2001)
2. V.F. Kitaeva, N.N. Sobolev, A.S. Zolot'ko, Mol. Cryst. Liq. Cryst., **91**, pp 137-143 (1983)
3. I.C. Khoo, M.V. Wood, B.D. Guenther, M-Y. Shih, P.H. Chen, Opt. Express, **2**,12, pp 471-482 (1998)
4. F. Derrien, J.F. Henninot, M. Warenghem, G. Abbate, J. Opt. A: Pure Appl. Opt. 2, pp332-337 (2000)
5. J.F. Henninot, M. Debailleul, F. Derrien, G. Abbate, M. Warenghem, Synt. Met. 124/1,pp 9-13, (2001)
6. D.J. Mitchell, A.W. Snyder, J.Opt. Soc. Am. B, **16**, 2, pp 236-239 (1999)
7. D.J. Mitchell et al, Phys. Rev. lett., **77**, 2, pp 271-273 (1996)
8. W. Krolikowsky, O. Bang, Phys. Rev. E, **63**, 016610 (2000)
9. H. Ono, Y. Harato, J.Opt. Soc. Am. B, **16**, 12, pp 2195-2201 (1999)